Research Article

Jun-Sheng Duan* and Yun-Yun Xu

Vibration Equation of Fractional Order Describing Viscoelasticity and Viscous Inertia

https://doi.org/10.1515/phys-2019-0088
Received Sep 09, 2019; accepted Nov 10, 2019

Abstract: The steady state response of a fractional order vibration system subject to harmonic excitation was studied by using the fractional derivative operator ${}_{-\infty}D_t^{\beta}$, where the order β is a real number satisfying $0 \le \beta \le 2$. We derived that the fractional derivative contributes to the viscoelasticity if $0 < \beta < 1$, while it contributes to the viscous inertia if $1 < \beta < 2$. Thus the fractional derivative can represent the "spring-pot" element and also the "inerter-pot" element proposed in the present article. The viscosity contribution coefficient, elasticity contribution coefficient, inertia contribution coefficient, amplitude-frequency relation, phase-frequency relation, and influence of the order are discussed in detail. The results show that fractional derivatives are applicable for characterizing the viscoelasticity and viscous inertia of materials.

Keywords: fractional derivative, viscoelasticity, viscous inertia, vibration

PACS: 02.30.Hq; 83.60.Bc; 46.35.+z; 46.40.-f

1 Introduction

Fractional calculus is a generalization and extension of integer order calculus and is applied to practical problems in science and engineering, including viscoelastic theory, anomalous diffusion, analysis of feedback amplifiers, fractal dynamics, fitting of experimental data and so forth [1–6]. Due to the widespread application of polymer materials in various fields of engineering, viscoelastic theory has undergone considerable development and constitutes one of the most successful application fields of fractional calculus.

The major merit of fractional calculus lies in the fact that it is a very suitable tool for the description of the memory and hereditary properties of various materials and processes [5–7]. It has been found that in many practical cases, systems can be more adequately described by using fractional order differential equations.

Scott-Blair [8, 9] proposed a fractional order constitutive equation $\sigma(t) = b\,{}_0D_t^{\nu}\epsilon(t)$ to describe the stress-strain relationship of viscoelastic materials, where $0 < \nu < 1$. Such an equation characterizes both the elasticity and the viscosity, so it represents a "spring-pot" element [10]. Based on this, studies of fractional oscillators and dynamical systems has attracted the interest of some scholars [11–20]. In [11], The equivalent integer order forms for three classes of fractional oscillators were considered. In [19], fractional calculus was introduced to model a class of memory oscillators. Some nonlinear fractional oscillators were investigated in [12, 13, 16, 20, 21]. The eigenvalues and eigenvector derivatives of fractional vibration systems were discussed in [22].

The concept of the inerter was proposed by Smith [23]. The inerter has two end points, one of which can move relative to the other. The magnitude of the force depends on the relative acceleration of the two end points. The inerter has been used in many fields, such as in the design of construction and suspension in racing cars, trains, ships, etc. [24–27].

In this article, we consider a fractional vibration system with fractional order β satisfying $0 \le \beta \le 2$, a greater range than that considered in previous work. By analyzing the steady state response, we explain that when the order satisfies $1 < \beta < 2$, the fractional derivative describes behavior of both spring pot and inerter. We suggest that the fractional element for an order $1 < \beta < 2$ corresponds to an "inerter-pot".

2 Basic concepts

Let the function $f(t)$ be piecewise continuous on $(a, +\infty)$ and integrable on any subinterval (a, t). The Riemann-

***Corresponding Author: Jun-Sheng Duan:** School of Sciences, Shanghai Institute of Technology, Shanghai 201418, China; Email: duanjs@sit.edu.cn
Yun-Yun Xu: School of Sciences, Shanghai Institute of Technology, Shanghai 201418, China; Email: xyuny1995@163.com

Liouville fractional integral of $f(t)$ is defined as

$$ {}_aJ_t^\beta f(t) := \int_a^t \frac{(t-s)^{\beta-1}}{\Gamma(\beta)} f(s)ds,\ \beta > 0 \tag{1} $$

where $\Gamma(\cdot)$ is the gamma function of Euler

$$ \Gamma(z) = \int_0^{+\infty} e^{-u}u^{z-1}du,\ z > 0. \tag{2} $$

Let $f^{(n)}(t)$ be piecewise continuous on $(a, +\infty)$ and integrable on any subinterval (a, t). Then the Caputo fractional derivative of $f(t)$ of order β $(n-1 < \beta < n)$ is defined as

$$ {}_aD_t^\beta f(t) := {}_aJ_t^{n-\beta} f^{(n)}(t),\ n-1 < \beta < n,\ n \in N^+. \tag{3} $$

If β is a non-negative integer, ${}_aD_t^\beta f(t)$ will be used to represent the integer order derivative $f^{(\beta)}(t)$.

In the following, we take $a = -\infty$, and use the fractional order operator ${}_{-\infty}D_t^\beta f(t)$ to study the steady state response of the fractional-order system under harmonic excitation.

3 Steady-state vibration with fractional derivative

Consider a fractional order vibration system with excitation in the form of the complex exponential function:

$$ m\ddot{x} + kx + c\dot{x} + G\,{}_{-\infty}D_t^\beta x = F_0 e^{\mathrm{i}\omega t}, \tag{4} $$

where $G\,{}_{-\infty}D_t^\beta x$ indicates a force associated with the entire deformation history for the viscoelastic material, m, k, c, G, F_0, ω are positive real constants, i is the imaginary unit and the order β is restricted to the interval $0 \le \beta \le 2$.

Similar to the case of integer orders, the form of the response is assumed to be

$$ x(t) = Xe^{\mathrm{i}\omega t}, \tag{5} $$

where X is the complex amplitude, independent of t. The integer order derivatives and the fractional derivative are calculated to be [2]

$$ \dot{x}(t) = X\mathrm{i}\omega e^{\mathrm{i}\omega t},\ \ddot{x}(t) = -X\omega^2 e^{\mathrm{i}\omega t}, \tag{6} $$

and

$$ {}_{-\infty}D_t^\beta x(t) = X(\mathrm{i}\omega)^\beta e^{\mathrm{i}\omega t}. \tag{7} $$

Substituting the first order derivative $\dot{x}(t)$, the second order derivative $\ddot{x}(t)$ and the fractional derivative in the above formulae into Eq. (4), we have

$$ -mX\omega^2 e^{\mathrm{i}\omega t} + kXe^{\mathrm{i}\omega t} + \mathrm{i}c\omega Xe^{\mathrm{i}\omega t} + G\,{}_{-\infty}D_t^\beta Xe^{\mathrm{i}\omega t} = F_0 e^{\mathrm{i}\omega t}. \tag{8} $$

Solving for the amplitude leads to

$$ X = \frac{F_0}{k - m\omega^2 + \mathrm{i}c\,\omega + G(\mathrm{i}\omega)^\beta}. \tag{9} $$

Using the equality

$$ \mathrm{i}^\beta = e^{\mathrm{i}\pi\beta/2} = \cos(\pi\beta/2) + \mathrm{i}\sin(\pi\beta/2), \tag{10} $$

we obtain the complex amplitude as

$$ X = \frac{F_0}{k - m\omega^2 + G\omega^\beta\cos(\pi\beta/2) + \mathrm{i}\left[c\,\omega + G\omega^\beta\sin(\pi\beta/2)\right]}. \tag{11} $$

In order to simplify the above formula, we assume that

$$ \begin{aligned} P &= k - m\omega^2 + G\omega^\beta\cos(\pi\beta/2), \\ Q &= c\,\omega + G\omega^\beta\sin(\pi\beta/2), \end{aligned} \tag{12} $$

and rewrite the complex amplitude into

$$ X = \frac{F_0}{P + Q\mathrm{i}}, \tag{13} $$

where $Q > 0$ is always true due to $0 \le \beta \le 2$. Introducing the phase difference ϕ to rewrite the complex amplitude, we have

$$ X = \frac{F_0 e^{-\mathrm{i}\phi}}{\sqrt{P^2 + Q^2}}, \tag{14} $$

where the phase difference between the excitation and the response is

$$ \phi = \begin{cases} \arctan(Q/P), & P > 0, \\ \pi/2, & P = 0, \\ \pi + \arctan(Q/P), & P < 0. \end{cases} \tag{15} $$

Thus, the response of the system to complex harmonic excitation is

$$ x(t) = \frac{F_0 e^{\mathrm{i}(\omega t - \phi)}}{\sqrt{\left[k - m\omega^2 + G\omega^\beta\cos(\pi\beta/2)\right]^2 + \left[c\,\omega + G\omega^\beta\sin(\pi\beta/2)\right]^2}}. \tag{16} $$

If $\beta = 0, 1, 2$, the fractional derivative contributes pure elasticity, viscosity, and inertia, respectively.

If $0 < \beta < 1$, we have $\cos(\pi\beta/2) > 0$ and $\sin(\pi\beta/2) > 0$. The fractional derivative contributes both to the damping and the stiffness. The solution of the original fractional order vibration system (4) is equivalent to the solution of the integer order system

$$ m\ddot{x} + \tilde{k}x + \tilde{c}\dot{x} = F_0 e^{\mathrm{i}\omega t}, \tag{17} $$

where

$$\tilde{k} = k + G\omega^{\beta}\cos(\pi\beta/2)\,,\ \tilde{c} = c + G\omega^{\beta-1}\sin(\pi\beta/2)\,. \quad (18)$$

Accordingly, the contributions of the fractional derivative term ${}_{-\infty}D_t^{\beta}x$ to damping and stiffness are

$$\tilde{c} - c = G\omega^{\beta-1}\sin(\pi\beta/2)\,,\ \tilde{k} - k = G\omega^{\beta}\cos(\pi\beta/2)\,. \quad (19)$$

If $1 < \beta < 2$, then we have $\cos(\pi\beta/2) < 0$, $\sin(\pi\beta/2) > 0$. The fractional derivative contributes both to the damping and the mass. The solution of the original fractional order vibration system (4) is equivalent to the solution of the integer order system

$$\tilde{m}\ddot{x} + kx + \tilde{c}\dot{x} = F_0 e^{i\omega t}, \quad (20)$$

where

$$\tilde{c} = c + G\omega^{\beta-1}\sin(\pi\beta/2)\,, \quad (21)$$
$$\tilde{m} = m - G\omega^{\beta-2}\cos(\pi\beta/2)\,.$$

So the contributions of the fractional derivative term ${}_{-\infty}D_t^{\beta}x$ to damping and mass are

$$\tilde{c} - c = G\omega^{\beta-1}\sin(\pi\beta/2)\,, \quad (22)$$
$$\tilde{m} - m = -G\omega^{\beta-2}\cos(\pi\beta/2)\,.$$

We call $(\tilde{c} - c)/G$, $(\tilde{k} - k)/G$ and $(\tilde{m} - m)/G$ the viscosity contribution coefficient, elasticity contribution coefficient and inertia contribution coefficient, respectively. They have the forms

$$(\tilde{c} - c)/G = \omega^{\beta-1}\sin(\pi\beta/2)\,,\ 0 < \beta < 2, \quad (23)$$
$$(\tilde{k} - k)/G = \omega^{\beta}\cos(\pi\beta/2)\,,\ 0 < \beta < 1, \quad (24)$$
$$(\tilde{m} - m)/G = -\omega^{\beta-2}\cos(\pi\beta/2)\,,\ 1 < \beta < 2. \quad (25)$$

The three contribution coefficients depend on both the excitation frequency ω and the fractional order β. For $0 < \beta < 1$, the viscosity contribution coefficient $(\tilde{c} - c)/G$ decreases with increase in ω, while for $1 < \beta < 2$, the coefficient $(\tilde{c} - c)/G$ increases with increase in ω. The elasticity contribution coefficient $(\tilde{k} - k)/G$ is defined on $0 < \beta < 1$, and is an increasing function of ω. The inertia contribution coefficient $(\tilde{m} - m)/G$ exists on $1 < \beta < 2$, and is a decreasing function of ω.

In Figure 1, the curves of the viscosity contribution coefficient $(\tilde{c} - c)/G$ versus the order β are shown on the interval $0 \le \beta \le 2$ for different values of ω. From Eq. (23) we deduce that the two curves for the values of ω which have a reciprocal relation are symmetric with respect to the straight line $\beta = 1$ as shown in Figure 1. For further analysis, we calculate the derivative as

$$\frac{d}{d\beta}\left[\omega^{\beta-1}\sin\left(\frac{\pi}{2}\beta\right)\right] = \omega^{\beta-1}\sin\left(\frac{\pi}{2}\beta\right)\ln(\omega) + \frac{\pi}{2}\omega^{\beta-1}\cos\left(\frac{\pi}{2}\beta\right). \quad (26)$$

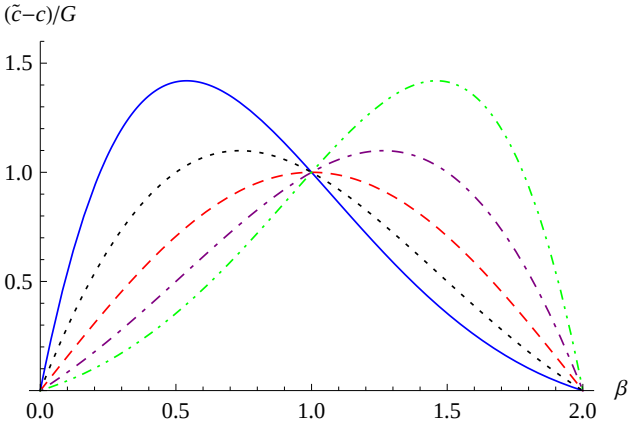

Figure 1: Curves of $(\tilde{c} - c)/G$ versus β on $0 \le \beta \le 2$ when ω takes different values: $\omega = 0.25$ (solid line), $\omega = 0.5$ (dotted line), $\omega = 1$ (dashed line), $\omega = 2$ (dot-dashed line), $\omega = 4$ (dot-dot-dashed line).

It can be concluded that $\omega^{\beta-1}\sin(\pi\beta/2)$ always increases and then decreases with β increasing from 0 to 2. At the stationary point

$$\beta^* = \frac{2}{\pi}\operatorname{arccot}\left[-\frac{2\ln(\omega)}{\pi}\right], \quad (27)$$

or equivalently,

$$\beta^* = \begin{cases} \frac{2}{\pi}\arctan\left[-\frac{\pi}{2\ln(\omega)}\right], & 0 < \omega < 1, \\ 1, & \omega = 1, \\ 2 - \frac{2}{\pi}\arctan\left[\frac{\pi}{2\ln(\omega)}\right], & \omega > 1, \end{cases} \quad (28)$$

the viscosity contribution coefficient $(\tilde{c} - c)/G$ takes the maximum

$$\left(\frac{\tilde{c} - c}{G}\right)^* = \omega^{\beta^*-1}\sin\left(\frac{\pi}{2}\beta^*\right). \quad (29)$$

The stationary point and the maximum depend on the frequency ω. Figures 2 and 3 show how their curves vary with the frequency ω, where the horizontal axes adopt the logarithmic scales in order to magnify the interval $0 < \omega < 1$ for visualization of the symmetrical patterns.

For $\omega = 1$, the stationary point lies at the midpoint $\beta^* = 1$ in Figures 1 and 2, and the maximum $[(\tilde{c} - c)/G]^*$ has the minimum 1 in Figures 1 and 3. With increase of ω on the interval $(0, +\infty)$, the stationary point β^* increases monotonically through the interval $(0, 2)$. The maximum $[(\tilde{c} - c)/G]^*$ approaches infinity as $\omega \to 0^+$ or $\omega \to +\infty$.

The curves of $(\tilde{k} - k)/G$ versus β on the interval $0 \le \beta \le 1$ for different values of ω are plotted in Figure 4. For further analysis, we consider the derivative

$$\frac{d}{d\beta}\left[\omega^{\beta}\cos\left(\frac{\pi}{2}\beta\right)\right] = \omega^{\beta}\cos\left(\frac{\pi}{2}\beta\right)\ln(\omega) - \frac{\pi}{2}\omega^{\beta}\sin\left(\frac{\pi}{2}\beta\right). \quad (30)$$

It can be concluded that if $0 < \omega \le 1$, the elasticity contribution coefficient $(\tilde{k} - k)/G$ decreases monotonically

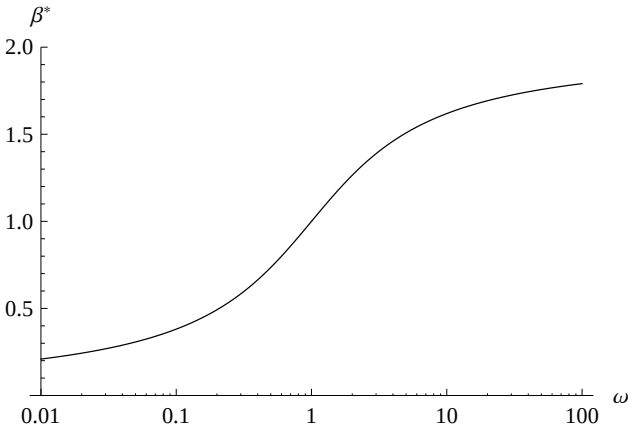

Figure 2: Curve of stationary point β^* versus ω.

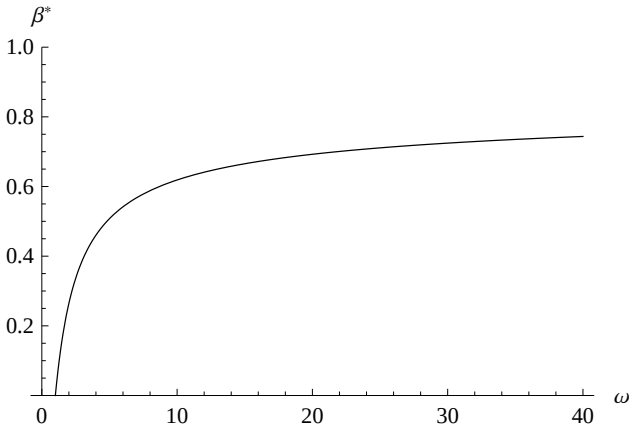

Figure 5: Curve of stationary point β^* versus ω.

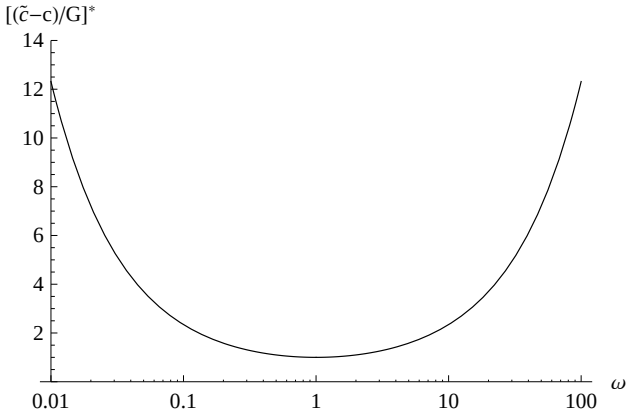

Figure 3: Curve of the maximum $\left[(\tilde{c}-c)/G\right]^*$ versus ω.

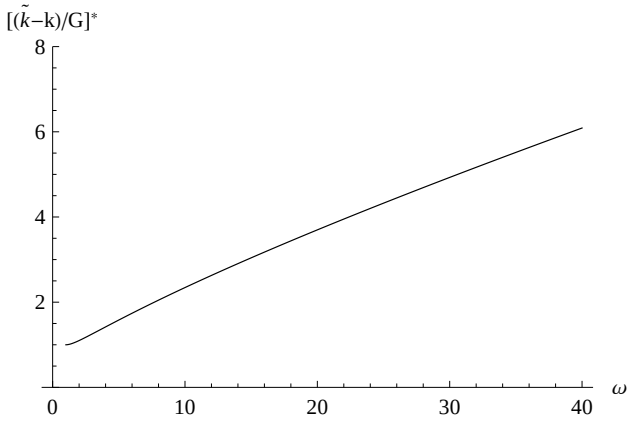

Figure 6: Curve of the maximum $[(\tilde{k}-k)/G]^*$ versus ω.

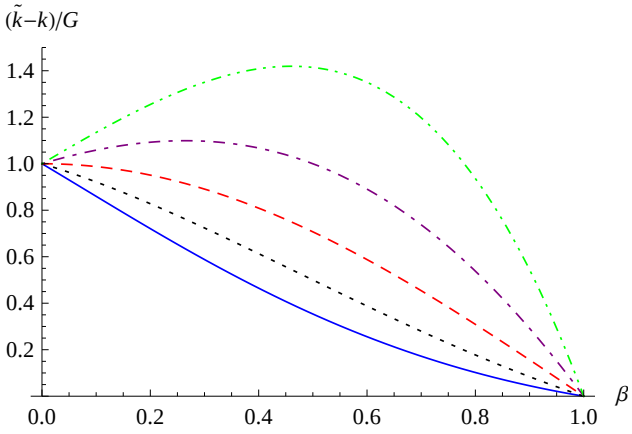

Figure 4: Curves of $(\tilde{k}-k)/G$ versus β on the interval $0 \le \beta \le 1$ when ω takes different values: $\omega = 0.25$ (solid line), $\omega = 0.5$ (dotted line), $\omega = 1$ (dashed line), $\omega = 2$ (dot-dashed line), $\omega = 4$ (dot-dot-dashed line).

with β increasing, while if $\omega > 1$ it has the maximum

$$\left(\frac{\tilde{k}-k}{G}\right)^* = \omega^{\beta^*}\cos\left(\frac{\pi}{2}\beta^*\right), \tag{31}$$

at the stationary point

$$\beta^* = \frac{2}{\pi}\arctan\left[\frac{2}{\pi}\ln(\omega)\right]. \tag{32}$$

In Figures 5 and 6, the curves of the stationary point β^* and the maximum $[(\tilde{k}-k)/G]^*$ versus the frequency ω on the interval $1 < \omega < 40$ are shown. With increase of ω on the interval $(1, +\infty)$, β^* increases monotonically through the interval $(0, 1)$, and the maximum $[(\tilde{k}-k)/G]^*$ increases monotonically through the interval $(1, +\infty)$.

In Figure 7, the curves of $(\tilde{m}-m)/G$ versus β on the interval $1 \le \beta \le 2$ are displayed for different values of ω. By calculating and analyzing the derivative

$$\frac{d}{d\beta}\left[-\omega^{\beta-2}\cos\left(\frac{\pi}{2}\beta\right)\right] = \omega^{\beta-2}\frac{\pi}{2}\sin\left(\frac{\pi}{2}\beta\right) - \omega^{\beta-2}\ln(\omega)\cos\left(\frac{\pi}{2}\beta\right), \tag{33}$$

we conclude that if $0 < \omega < 1$, the inertia contribution coefficient $(\tilde{m}-m)/G$ always first increases and then decreases on the interval $1 \le \beta \le 2$, reaching the maximum

$$\left(\frac{\tilde{m}-m}{G}\right)^* = -\omega^{\beta^*-2}\cos\left(\frac{\pi}{2}\beta^*\right), \tag{34}$$

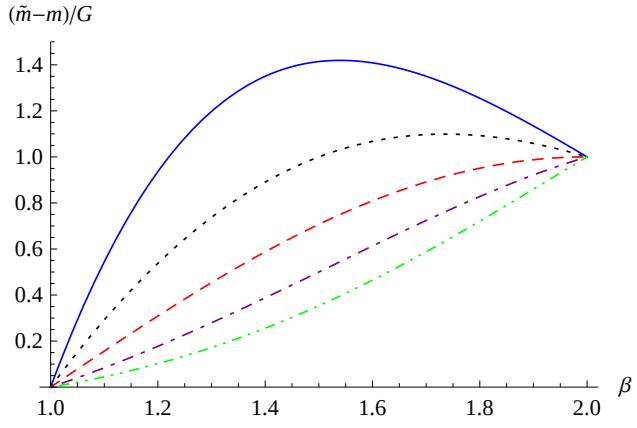

Figure 7: Curves of $(\tilde{m}-m)/G$ versus β on the interval $1 \le \beta \le 2$ when ω takes different values: $\omega = 0.25$ (solid line), $\omega = 0.5$ (dotted line) $\omega = 1$ (dashed line), $\omega = 2$ (dot-dashed line), $\omega = 4$ (dot-dot-dashed line).

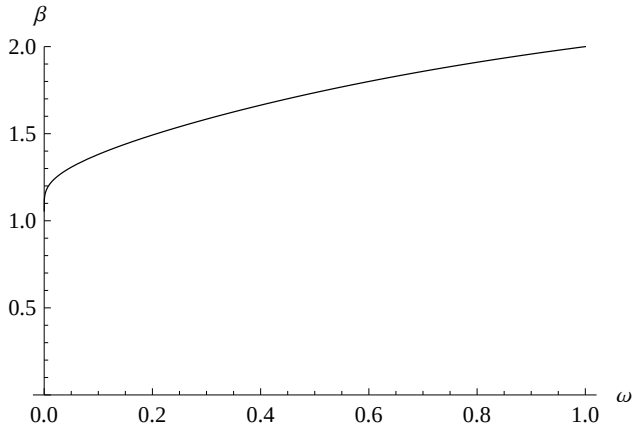

Figure 8: Curve of stationary point β^* versus ω.

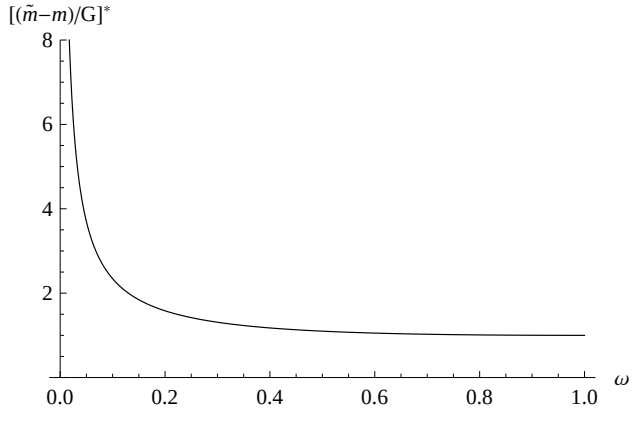

Figure 9: Curve of the maximum $\left[(\tilde{m}-m)/G\right]^*$ versus ω.

at the stationary point

$$\beta^* = 2+\frac{2}{\pi}\arctan\left[\frac{2}{\pi}\ln(\omega)\right], \tag{35}$$

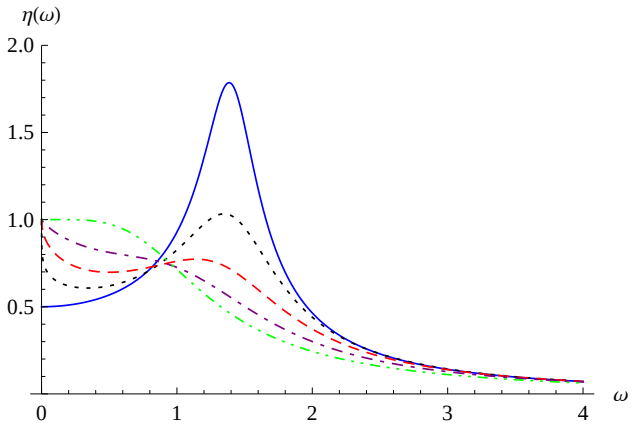

Figure 10: For $m = k = G = 1$, $c = 0.4$, curves of $\eta(\omega)$ versus ω when β takes the values: $\beta = 0$ (solid line), $\beta = 0.25$ (dotted line), $\beta = 0.5$ (dashed line), $\beta = 0.75$ (dot-dashed line), $\beta = 1$ (dot-dot-dashed line).

while if $\omega \ge 1$, the inertia contribution coefficient $(\tilde{m}-m)/G$ increases monotonically with increase in β.

In Figures 8 and 9, the curves of the stationary point β^* and the maximum $\left[(\tilde{m}-m)/G\right]^*$ versus the frequency ω on the interval $0 < \omega < 1$ are shown. With increase in ω on the interval $(0, 1)$, the stationary point β^* increases monotonically through the interval $(1, 2)$, and the maximum $\left[(\tilde{m}-m)/G\right]^*$ decreases monotonically through the interval $(1, +\infty)$.

Next, we consider the amplitude-frequency and phase-frequency relations. From Eq. (16), the amplitude amplification factor is derived as a function of ω,

$$\eta(\omega) = \frac{|x(t)|}{F_0/k} = \frac{k}{\sqrt{\left[k-m\omega^2+G\omega^\beta\cos(\pi\beta/2)\right]^2+\left[c\,\omega+G\omega^\beta\sin(\pi\beta/2)\right]^2}}. \tag{36}$$

Also, the phase difference in Eq. (15) is regarded as a function of the frequency ω,

$$\phi(\omega) = \begin{cases} \arctan\frac{c\,\omega+G\omega^\beta\sin(\pi\beta/2)}{k-m\omega^2+G\omega^\beta\cos(\pi\beta/2)}, & P > 0, \\ \pi/2, & P = 0, \\ \pi+\arctan\frac{c\,\omega+G\omega^\beta\sin(\pi\beta/2)}{k-m\omega^2+G\omega^\beta\cos(\pi\beta/2)}, & P < 0, \end{cases} \tag{37}$$

where $P = k - m\omega^2 + G\omega^\beta\cos(\pi\beta/2)$. Take $m = k = G = 1$, $c = 0.4$. The amplitude-frequency curves $\eta(\omega)$ are shown in Figures 10 and 11, and the phase-frequency curves $\phi(\omega)$ are shown in Figures 12 and 13, where the order β takes different values 0, 0.25, 0.5, 0.75, 1, 1.25, 1.5, 1.75 and 2.

We note that the limit $\lim_{\omega\to 0^+}\eta(\omega)$, as a function of β, has a jump between $\beta = 0$ and $\beta > 0$ (see Figure 10). For $0 < \beta < 1$, small damping corresponds to $\tilde{c}^2 - 4m\tilde{k} < 0$ in Eq. (17). For $1 < \beta < 2$, small damping corresponds to

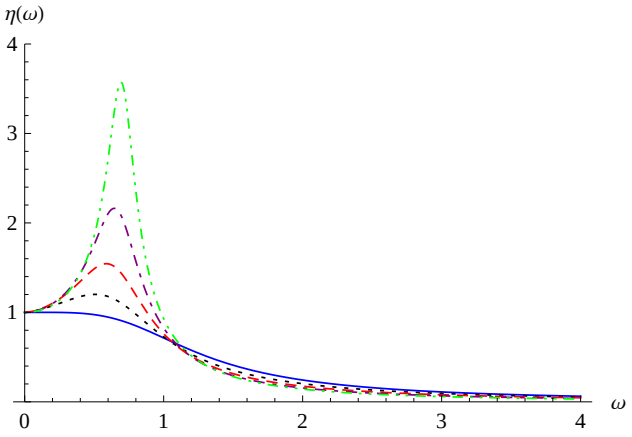

Figure 11: For $m = k = G = 1$, $c = 0.4$, curves of $\eta(\omega)$ versus ω when β takes the values: $\beta = 1$ (solid line), $\beta = 1.25$ (dotted line), $\beta = 1.5$ (dashed line), $\beta = 1.75$ (dot-dashed line), $\beta = 2$ (dot-dot-dashed line).

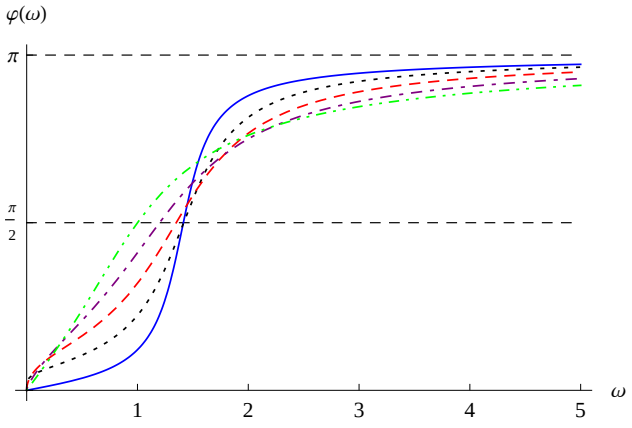

Figure 12: For $m = k = G = 1$, $c = 0.4$, curves of $\phi(\omega)$ versus ω when β takes the values: $\beta = 0$ (solid line), $\beta = 0.25$ (dotted line), $\beta = 0.5$ (dashed line), $\beta = 0.75$ (dot-dashed line), $\beta = 1$ (dot-dot-dashed line).

$\tilde{c}^2 - 4\tilde{m}k < 0$ in Eq. (20). For the case under considerationn, $m = k = G = 1$, $c = 0.4$, the system has obvious small damping as β approaches 0 or 2. So the amplitude-frequency curves $\eta(\omega)$ display distinct resonance peaks in Figures 10 and 11. The resonance peaks descend with increase of β from 0 to 1 in Figure 10, while the peaks ascend with increase of β from 1 to 2 in Figure 11.

In Figures 12 and 13, variations of excitation and response from in-phase to anti-phase are displayed as ω increases. Moderate transitions from in-phase to anti-phase are shown as β approaches 1, while sharp transitions appear for β approaching 0 or 2, the case of small damping.

Finally, we consider the quality factor of the oscillatory system. If $0 < \beta < 1$, from Eq. (17) the equivalent damping ratio is

$$\zeta = \frac{\tilde{c}}{2\sqrt{m\tilde{k}}}.$$

For smaller damping (usually $\zeta < 0.05$), the amplitude amplification factor at resonant frequency is the quality factor, which is approximated as $Q = 1/(2\zeta)$, $0 < \beta < 1$. If $1 < \beta < 2$, from Eq. (20) the equivalent damping ratio is

$$\zeta = \frac{\tilde{c}}{2\sqrt{\tilde{m}k}}.$$

The quality factor is $Q = 1/(2\zeta)$, $1 < \beta < 2$. The quality factor can effectively reflect the damping strength of an oscillatory system. A peculiar aspect is that these quantities are related to the frequency ω.

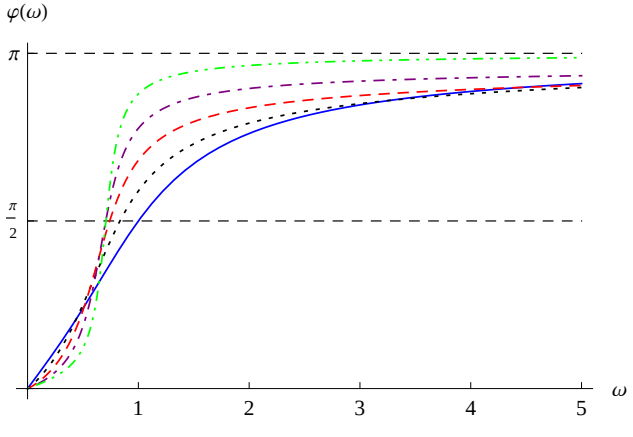

Figure 13: For $m = k = G = 1$, $c = 0.4$, curves of $\phi(\omega)$ versus ω when β takes the values: $\beta = 1$ (solid line), $\beta = 1.25$ (dotted line), $\beta = 1.5$ (dashed line), $\beta = 1.75$ (dot-dashed line), $\beta = 2$ (dot-dot-dashed line).

4 Conclusion

In this paper, the steady state response of fractional order vibration systems under harmonic excitation was studied by using the fractional derivative operator ${}_{-\infty}D_t^{\beta}$. We used the harmonic excitation in the form of a complex exponential function to discuss the contribution of the fractional derivative term to the damping, stiffness and mass, respectively. If $\beta = 0, 1, 2$, the fractional derivative contributes pure elasticity, viscosity, and inertia, respectively.

We derived that if $0 < \beta < 1$, the fractional derivative term causes contributions to damping and stiffness, so it characterizes viscoelasticity and represents a “spring-pot” element; if $1 < \beta < 2$, the fractional derivative term produces contributions to damping and mass, so it characterizes viscous inertia and represents an “inerter-pot”, which

is a newly proposed terminology in this paper. Dependencies of the viscosity contribution coefficient, elasticity contribution coefficient and inertia contribution coefficient, respectively, on the frequency ω and the order β were investigated. We also discussed the amplitude-frequency relation, the phase-frequency relation and the influence of the order. The results show that fractional derivatives are applicable for describing the viscoelasticity and viscous inertia of materials.

Acknowledgements

This work was supported by the National Natural Science Foundation of China (No.11772203) and the Natural Science Foundation of Shanghai (No.17ZR1430000).

References

[1] Miller K.S., Ross B., An Introduction to the Fractional Calculus and Fractional Differential Equations, Wiley, New York, 1993.
[2] Podlubny I., Fractional Differential Equations, Academic, San Diego, 1999.
[3] Kilbas A.A., Srivastava H.M., Trujillo J.J., Theory and Applications of Fractional Differential Equations, Elsevier, Amsterdam, 2006.
[4] Li M., Fractal time series – a tutorial review, Math. Probl. Eng., 2010, 2010, 157264 (26 pages).
[5] Mainardi F., Fractional Calculus and Waves in Linear Viscoelasticity, Imperial College, London, 2010.
[6] Butzer P.L., Westphal U., An Introduction to Fractional Calculus, World Scientific, Singapore, 2000.
[7] Rossikhin Y.A., Shitikova M.V., Applications of fractional calculus to dynamic problems of linear and nonlinear hereditary mechanisms of solids, Appl. Mech. Rev., 1997, 50, 15-67.
[8] Scott-Blair G.W.S., The role of psychophysics in rheology, J. Colloid Sciences, 1947, 2, 21-32.
[9] Scott-Blair G.W.S., Analytical and integrative aspects of the stress-strain-time problem, J. Scientific Instruments, 1944, 21, 80-84.
[10] Koeller R.C., Applications of fractional calculus to the theory of viscoelasticity, J. Appl. Mech., 1984, 51, 299-307.
[11] Li M., Three classes of fractional oscillators, Symmetry, 2018, 10, 40 (91 pages).
[12] Gafiychuk V., Datsko B., Stability analysis and limit cycle in fractional system with Brusselator nonlinearities, Phys. Lett. A, 2008, 372, 4902-4904.
[13] Attari M., Haeri M., Tavazoei M.S., Analysis of a fractional order Van der Pol-like oscillator via describing function method, Nonlinear Dynam., 2010, 61, 265-274.
[14] Baleanu D., Diethelm K., Scalas E., Trujillo J.J., Fractional Calculus Models and Numerical Methods (Series on Complexity, Nonlinearity and Chaos), World Scientific, Boston, 2012.
[15] Jafari H., Daftardar-Gejji V., Solving a system of nonlinear fractional differential equations using Adomian decomposition, J. Comput. Appl. Math., 2006, 196, 644-651.
[16] Wu G.C., Baleanu D., Xie H.P., Chen F.L., Chaos synchronization of fractional chaotic maps based on the stability condition, Physica A, 2016, 460, 374-383.
[17] Li C., Ma Y., Fractional dynamical system and its linearization theorem, Nonlinear Dynam., 2013, 71, 621-633
[18] Huang C., Duan J.S., Steady-state response to periodic excitation in fractional vibration system, J. Mech., 2016, 32, 25-33.
[19] Parovik R.I., Mathematical model of a wide class memory oscillators, Bulletin of the South Ural State University. Ser. Mathematical Modelling, Program. Comput. Soft., 2018, 11, 108-122.
[20] Parovik R.I., Amplitude-frequency and phase-frequency performances of forced oscillations of a nonlinear fractional oscillator, Tech. Phys. Lett., 2019, 45, 660-663.
[21] Duan J.S., Huang C., Liu L.L., Response of a fractional nonlinear system to harmonic excitation by the averaging method, Open Phys., 2015, 13, 177-182.
[22] Lin R.M., Ng T.Y., Eigenvalue and eigenvector derivatives of fractional vibration systems, Mech. Syst. Signal Pr., 2019, 127, 423-440.
[23] Smith M.C., Synthesis of mechanical networks: the inerter, IEEE Trans. Automat. Contr., 2002, 47, 1648-1662.
[24] Wang F.C., Liao M.K., Liao B.H., Su W.J., Chan H.A., The performance improvements of train suspension systems with mechanical networks employing inerters, Vehicle Syst. Dyn., 2009, 47, 805-830.
[25] Evangelou S., Limebeer D.J.N., Sharp R.S., Smith M.C., Control of motorcycle steering instabilities, IEEE Contr. Syst. Mag., 2006, 26, 78-88.
[26] Papageorgiou C., Smith M.C., Positive real synthesis using matrix inequalities for mechanical networks: application to vehicle suspension, IEEE Trans. Contr. Syst. Tech., 2006, 14, 423-435.
[27] Chen M.Z.Q., Hu Y., Huang L., Chen G., Influence of inerter on natural frequencies of vibration systems, J. Sound Vib., 2014, 333, 1874-1887.